Science and Technology Indonesia
e-ISSN:2580-4391 *p*-ISSN:2580-4405
Vol. 10, No. 3, July 2025

Research Paper

High Surface Area *Ortho*-Nb_2O_5 as Bifunctional Adsorbent and Photocatalyst for Efficient Removal of Tetracycline Antibiotics from Wastewater

Tarmizi Taher[1,2*], Putri Maharani[1], Sephia Amanda Muhtar[2], Andika Munandar[1], Ahmad Nur Sidiq[3], Aditya Rianjanu[2,4*]

[1]*Department of Environmental Engineering, Institut Teknologi Sumatera, Lampung, 35365, Indonesia*
[2]*Center for Green and Sustainable Materials, Institut Teknologi Sumatera, Lampung, 35365, Indonesia*
[3]*Department of Nutrition Science, Sriwijaya University, South Sumatera, 30139, Indonesia*
[4]*Department of Materials Engineering, Institut Teknologi Sumatera, Lampung Selatan, 35365, Indonesia*
***Corresponding author**: tarmizi.taher@tl.itera.ac.id; aditya.rianjanu@mt.itera.ac.id

Abstract
The presence of antibiotics in aquatic environments poses significant environmental and health risks, requiring advanced treatment strategies for their removal. In this study, we report the straightforward hydrothermal synthesis of high surface area *ortho*-Nb_2O_5 and its dual role as both an adsorbent and photocatalyst for the removal of tetracycline (TC) from wastewater. The structural and morphological properties of *ortho*-Nb_2O_5 were systematically investigated using XRD, FTIR, FESEM-EDS, and BET surface area analysis. The *ortho*-Nb_2O_5 synthesized at 72 hours (Nb_2O_5_72) exhibited a high BET surface area of 242.42 m^2/g, mesoporosity, and a bandgap of 3.28 eV, enabling efficient UV-driven photocatalysis. Adsorption studies revealed a high TC removal capacity of 32 mg/g at equilibrium. Under UV irradiation, *ortho*-Nb_2O_5 achieved significant photocatalytic degradation of TC.

Keywords
Ortho-Nb_2O_5, Photocatalysis, Adsorption, Hydrothermal Synthesis, Bifunctional Material, Tetracycline

Received: 7 February 2025, Accepted: 29 May 2025
https://doi.org/10.26554/sti.2025.10.3.916-923

1. INTRODUCTION

The extensive use of antibiotics in human and veterinary medicine has led to their widespread occurrence in various environmental compartments (Serwecińska, 2020; Almansour et al., 2021; Mishra et al., 2025; Thakur et al., 2025). Among these, tetracyclines (TC) represent one of the most frequently detected classes due to their broad-spectrum efficacy and persistence (Almansour et al., 2021). However, their environmental presence has raised significant concerns regarding public and ecological health. One of the most critical implications is the promotion of antibiotic-resistant bacteria (Hamdan et al., 2024). TC, even at subinhibitory concentrations, can exert selective pressure that promotes the emergence and propagation of resistance genes. This phenomenon not only undermines the efficacy of existing antimicrobial therapies but also poses a substantial risk to global public health (Haseeb et al., 2023).

Beyond resistance, tetracycline can disrupt native microbial communities in soil and aquatic environments, impairing vital ecological processes such as soil respiration and nitrification (Filliping et al., 2008). These disruptions can cascade through ecosystems, affecting nutrient cycling and biodiversity. Moreover, tetracycline has been associated with adverse effect on aquatic and terrestrial organisms, including endocrine disruption and other toxicological response (Daghrir and Drogui, 2013). The persistence of tetracycline is exacerbated by their chemical stability and resistance to biodegradation. With a reported half-life of approximately 500 days in soil, these compounds can accumulate over time, leading to long term contamination (Antos et al., 2024).

Conventional wastewater treatment systems are often inadequate for their removal, resulting in their continued release in the environment thought effluents form pharmaceutical industries, municipal sewage, and agricultural runoff (Nie et al., 2024). Therefore, several advanced treatment technologies are being investigated to mitigate TC contamination (Rivera-Utrilla et al., 2018). Methods such as advanced oxidation processes (AOPs), adsorption technique, and photocatalytic degradation have demonstrated potential in laboratory-scale studies (Koundle et al., 2024). However, these technologies require further development and optimization to ensure effectiveness and economic viability at industrial scales.

The presence of antibiotics in aquatic environments poses serious environmental and health risks, particularly due to their persistence and contribution to antibiotic resistance (Asif et al., 2024; Ni et al., 2024; Yao et al., 2024). Tetracycline (TC),

an antibiotic commonly used in both medical and veterinary applications, is frequently found in wastewater environments (Asif et al., 2024). TC is resistant to biodegradation, making it persistent in the environment and difficult to remove using conventional wastewater treatment systems, which leads to its accumulation in soil and water. Moreover, one of the most critical impacts of its presence is the promotion of antibiotic-resistant bacteria, which poses a significant threat to public health. Unfortunately, conventional water treatment methods often fail to completely remove TC, making it necessary to explore advanced degradation strategies (Yao et al., 2024). Among the commonly used methods (Taher et al., 2021a), photocatalysis has emerged as an effective and sustainable solution for wastewater treatment, as it can address complex and persistent organic contaminants (Saadati et al., 2016; Leong et al., 2022).

Recently, niobium pentoxide (Nb_2O_5) has emerged as a promising photocatalytic material due to its moderate bandgap (3.2 eV), high stability, and acid-functional surface (Ahmad et al., 2024). A distinct structural variant, known as *ortho*-Nb_2O_5, features a deformed orthorhombic crystalline structure composed of NbO_6 octahedra and Nb_6O_{21} pentagonal units forming microporous, nano-rod-shaped architectures. This material, hydrothermally synthesized from ammonium niobium oxalate, exhibits an exceptionally high surface area, abundant Brønsted and Lewis acid sites, and a unique combination of adsorption and photocatalytic properties (Nakajima et al., 2017). Our previous study demonstrated its bifunctional role as an efficient adsorbent and UV-active photocatalyst for methylene blue (MB) removal, with adsorption capacities exceeding 75 mg/g and complete photocatalytic regeneration under UV light (Taher et al., 2021b). However, its potential application in degrading more structurally complex and persistent pharmaceutical pollutants such as tetracycline (TC) has not yet been explored. Given its strong surface acidity, ion-exchange capability, and reusability, *ortho*-Nb_2O_5 represents a novel, underutilized photocatalyst platform for the mineralization of recalcitrant antibiotic residues in water environments.

In this work, we report the simple hydrothermal synthesis of *ortho*-Nb_2O_5 using ammonium niobium oxalate as a precursor and evaluate its bifunctional role as an adsorbent and photocatalyst for removing tetracycline from wastewater (Taher et al., 2021b). We systematically investigate the impact of synthesis conditions on the material's properties. We assessed the adsorption and photocatalytic performance to provide insights into Nb_2O_5's dual functionality in antibiotic removal. This study aims to establish Nb_2O_5 as a viable material for removing emerging contaminants from wastewater, contributing to the advancement of sustainable water treatment technologies.

2. EXPERIMENTAL SECTION

2.1 Materials

Ammonium niobium oxalate hydrate ($NH_4[Nb(O)(C_2O_4)_2(H_2O)_2]\cdot nH_2O$) was purchased from Sigma-Aldrich (Germany) and used as the niobium precursor without further purification. Tetracycline hydrochloride (TC) was obtained from Merck (Germany) and used as the target pollutant in adsorption and photocatalytic experiments. All other chemicals were of analytical grade and used as received. Deionized (DI) water was used throughout all synthesis and experimental procedures.

2.2 Hydrothermal Synthesis of *Ortho*-Nb_2O_5

The Nb2O5 was synthesized using the hydrothermal method described in previous literature (Nakajima et al., 2017). In brief, six mmol of ammonium niobium oxalate hydrate ($NH_4[Nb(O)(C_2O_4)_2(H_2O)_2]\cdot nH_2O$), Sigma-Aldrich, Germany) was dissolved in 40 mL of deionized water under vigorous stirring. The solution was then transferred to a Teflon-lined stainless-steel autoclave (100 mL capacity), which was heated at 175°C for a predetermined reaction time (24 – 72 hours). After cooling to room temperature, the resulting solid was filtered, washed several times with DI water, and dried overnight at 80°C.The obtained materials was labelled as Nb_2O_5_X, where X refers to the hydrothermal time.

2.3 Materials Characterization

The phase composition and crystallinity of the synthesized *ortho*-Nb_2O_5 were examined using X-ray diffraction (XRD) (Rigaku Smartlab and Cu-Kα radiation). Functional groups and surface chemistry were analyzed using FTIR (Shimadzu IR Spirit-X, Japan). Morphological and elemental characteristics were investigated through field-emission scanning electron microscopy (FESEM) coupled with energy-dispersive X-ray spectroscopy (EDS). Specific surface area, pore volume, and pore size distribution were determined using nitrogen adsorption-desorption isotherms based on the BET method with a Micromeritics ASAP 2020. Optical properties were assessed via UV-Vis diffuse reflectance spectroscopy (UV-Vis DRS) using a Shimadzu UV-2600, and the band gap energy was estimated through Tauc plot analysis.

2.4 Photocatalytic Degradation of Tetracycline

A custom photoreactor equipped with a UV lamp was used for adsorption and degradation studies. Photocatalytic experiments involved 100 mL of a tetracycline solution (10 mg/L) containing 0.1 g of Nb_2O_5 catalyst. The suspension was stirred magnetically in the dark for predetermined times to achieve adsorption-desorption equilibrium and was then exposed to UV light for up to 120 minutes. Aliquots were regularly withdrawn, filtered, and analyzed. The concentration of tetracycline in the solutions was measured using a UV-Vis spectrophotometer (Shimadzu UV-2600) at its maximum absorbance wavelength of 357 nm.

3. RESULTS AND DISCUSSION

3.1 Materials characterization

The phase composition and crystallinity of the synthesized *ortho*-Nb_2O_5 samples were evaluated by X-ray diffraction (XRD), and the results are shown in Figure 1a. All samples exhibit distinct diffraction peaks that match well with the orthorhombic

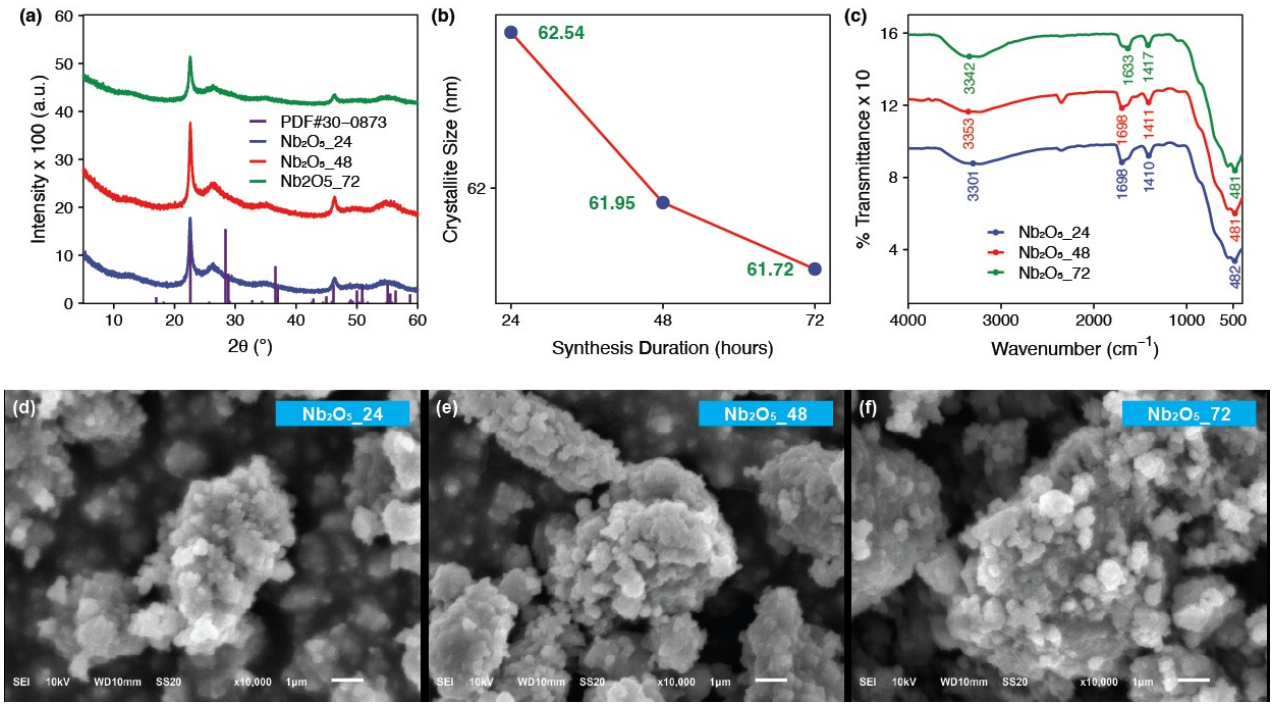

Figure 1. XRD Pattern (A), Crystallite Size Variation (B), FTIR Spectra (C), and SEM Images (D-F) of Nb_2O_5 Synthesized at Different Durations (24, 48, and 72 h)

Nb_2O_5 phase (JCPDS No. 30-0873) (Nakajima et al., 2017), indicating successful formation of the desired crystalline structure. The absence of impurity peaks further suggests high phase purity across all samples.

Prominent reflections at $2\theta \approx 22.7°$ and $45.2°$, corresponding to the (001) and (002) planes, respectively, are associated with the layered stacking along the c-axis of the orthorhombic structure (Rianjanu et al., 2024b). These planes are known to be indicative of the development of long-range order within the Nb_2O_5 lattice. As the hydrothermal synthesis time increases, the diffraction peaks become progressively sharper and more intense, reflecting an increase in crystallite size and overall structural ordering.

The average crystallite size of the *ortho*-Nb_2O_5 samples was estimated using the Scherrer equation based on the FWHM of the dominant (001) reflection, as shown in Figure 1b. A slight but consistent reduction in crystallite size was observed with increasing hydrothermal treatment time, suggesting a progressive refinement of crystalline domains. This trend may reflect the interplay between nucleation and growth kinetics under hydrothermal conditions, where extended durations promote the formation of more uniform and well-faceted crystallites.

Interestingly, the reduction in crystallite size with prolonged synthesis time can be correlated with enhanced surface area and a higher density of surface-active sites, both of which are favorable for catalytic applications. Smaller crystallite dimensions also shorten the diffusion path lengths for charge carriers, which can help suppress bulk recombination processes and improve photocatalytic efficiency (Wang et al., 2013). This observation aligns with previous reports that underscore the role of nanostructural control in optimizing the physicochemical properties of Nb_2O_5-based materials for photocatalytic and adsorption applications (Santos et al., 2021; Taher et al., 2021b; Ahmad et al., 2024).

The FTIR spectra (Figure 1c) display characteristic vibrational modes associated with Nb–O stretching, typically observed in the range of 800–1000 cm^{-1}, confirming the formation of Nb_2O_5 frameworks (Taher et al., 2021b). Broad absorption around 3400 cm^{-1} and a band near 1630 cm^{-1} are attributed to O–H stretching and bending vibrations, indicative of surface hydroxyl groups and adsorbed water. These hydroxyl species are known to influence surface reactivity and facilitate charge carrier trapping during photocatalysis. Subtle shifts in peak positions and intensities among the samples imply changes in the local bonding environment, likely induced by variations in crystallinity and surface hydroxylation resulting from different hydrothermal treatment durations.

The surface morphology of the synthesized *ortho*-Nb_2O_5 samples, observed via SEM (Figures 1d–f), reveals notable changes as a function of hydrothermal treatment time. The Nb_2O_5_24h sample displays irregularly shaped and loosely aggregated particles, indicative of incomplete crystal growth and limited particle fusion at shorter synthesis durations. In contrast, the Nb_2O_5_48h sample exhibits more defined and granular morphologies with visible textural porosity, suggesting improved nucleation and particle coalescence. At an ex-

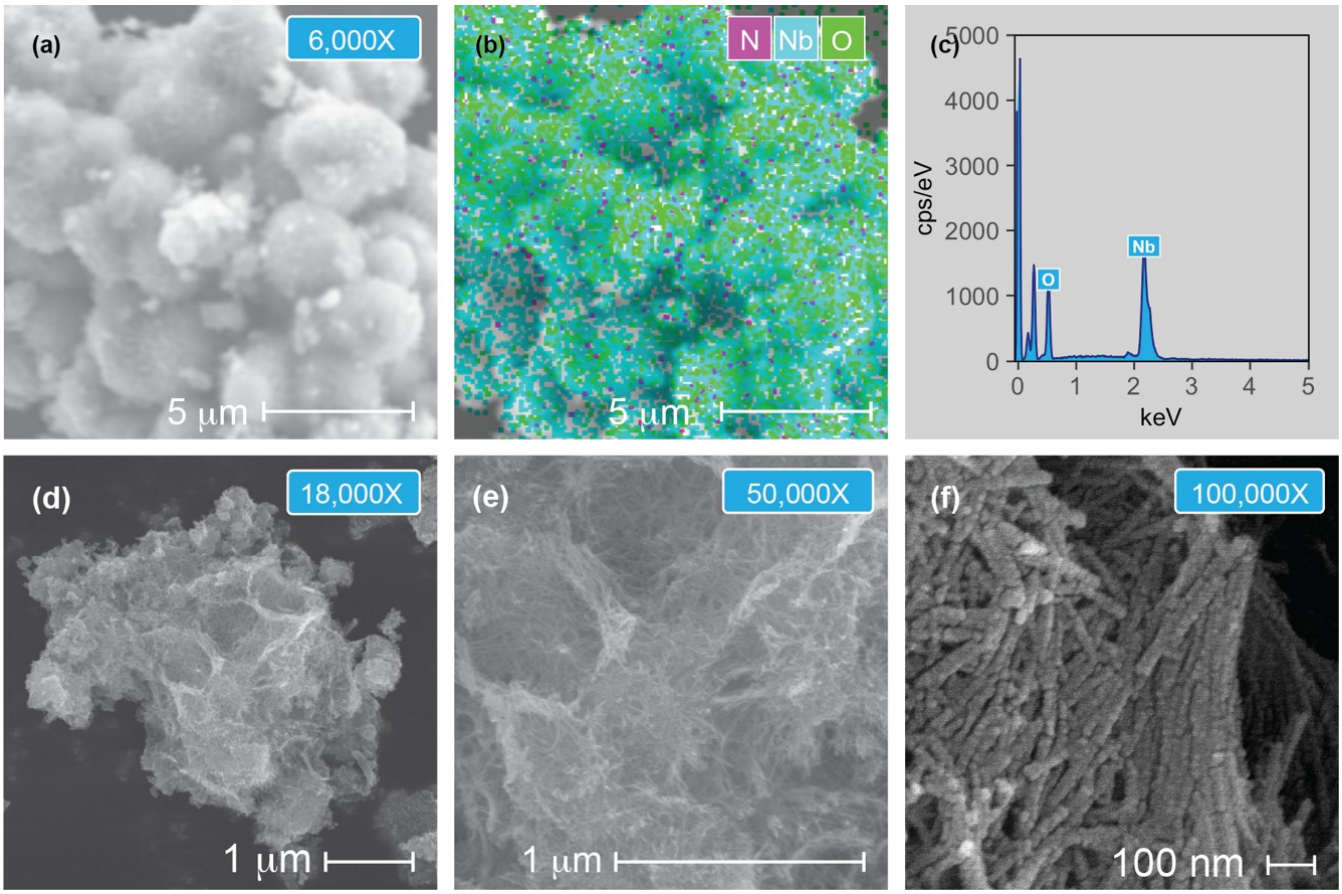

Figure 2. Surface Morphology and Elemental Composition of Nb_2O_5_72h Sample. (A) FESEM Image at 6,000× Magnification Showing Aggregated Particle Clusters. (B) Elemental Mapping Confirming the Homogeneous Distribution of Niobium (Nb), Oxygen (O), and Trace Nitrogen (N) Across the Sample Surface. (C) EDS Spectrum Indicating the Presence of Nb and O with No Detectable Impurities. (D–F) High-Magnification FESEM Images at 18,000×, 50,000×, And 100,000×, Respectively, Revealing Fibrous and Rod-Like Nanostructures with High Surface Roughness and Interparticle Porosity

tended duration of 72 hours, the Nb_2O_5_72h sample shows pronounced particle growth, with smoother surfaces and denser agglomeration, reflecting advanced crystal maturation and reduced surface defects.

This morphological evolution-shifting from loosely aggregated domains to more compact and interconnected particle networks-can significantly influence the surface area, pore structure, and interfacial contact with target molecules. Such features are particularly important for photocatalytic and adsorptive applications, where mass transfer and active site accessibility are critical. Given these observations, further analysis will focus on the Nb_2O_5_72h sample, which combines improved crystallinity and well-developed morphology, making it a promising candidate for advanced photocatalytic performance.

The surface morphology of the Nb_2O_5_72h sample was further examined using field emission scanning electron microscopy (FESEM) at various magnifications (Figures 2a, d–f). At lower magnification (6,000×, Figure 2a), the material appears as large, dense aggregates composed of interconnected nanoscale particles. Higher-magnification images (18,000× to 100,000×; Figures 3d–f) reveal a more detailed fibrous or rod-like morphology with well-developed surface texture and significant interparticle voids (Rianjanu et al., 2024a). The observed anisotropic nanostructures may facilitate improved surface area and enhance photocatalytic performance by promoting charge separation and providing more active sites for surface reactions.

Elemental mapping via energy-dispersive X-ray spectrosco py (EDS) confirms the homogeneous distribution of niobium (Nb) and oxygen (O) throughout the sample, with no signs of elemental segregation (Figure 2b). A minor signal for nitrogen (N) is also observed, possibly arising from residual precursors or environmental adsorption during sample handling. The corresponding EDS spectrum (Figure 2c) shows two dominant peaks at ~2.16 keV and ~0.52 keV, corresponding to Nb and O, respectively, further confirming the high purity of the Nb_2O_5 phase. The fibrous rod-like morphology, combined with uni-

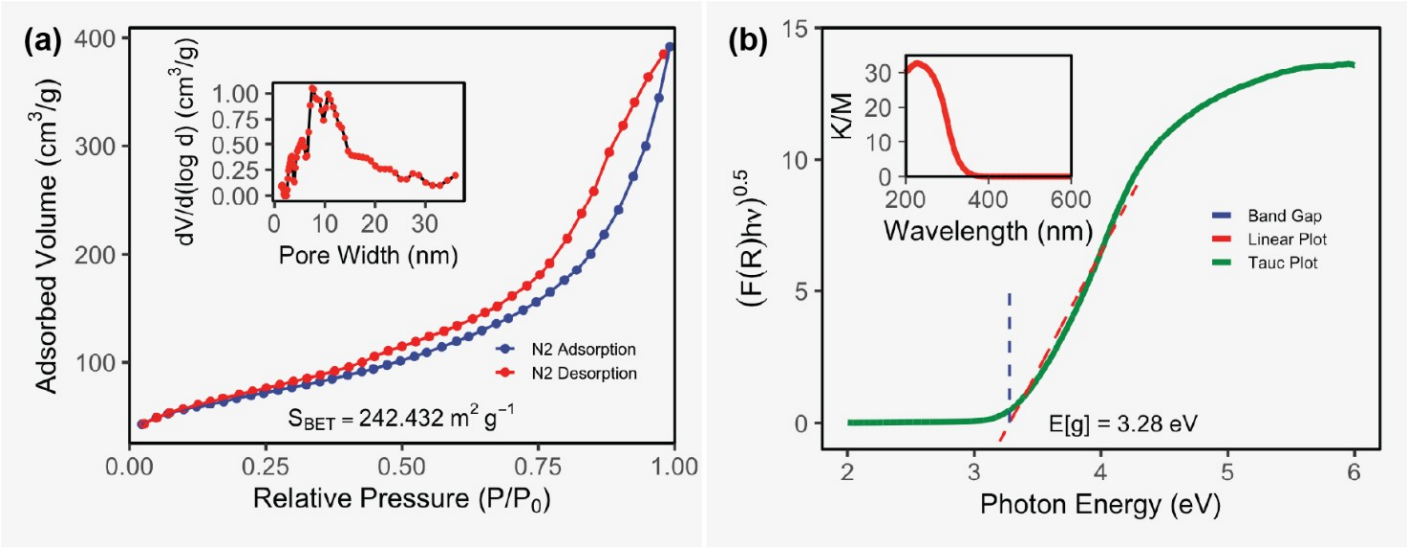

Figure 3. Textural and Optical Properties of Nb_2O_5_72h Sample. (A) Nitrogen Adsorption–Desorption Isotherm Showing A Type IV Hysteresis Loop, Characteristic of Mesoporous Structures. The Specific Surface Area Was Determined To Be 242.432 M^2 G^{-1} Based on BET Analysis. Inset: BJH Pore Size Distribution Showing Predominant Mesopores Centered Around 10–15 Nm. (B) Tauc Plot Derived from UV–Vis Diffuse Reflectance Spectra Used to Estimate the Optical Band Gap. The Extrapolated Linear Region Indicates A Band Gap Energy (Eg) Of 3.28 Ev. Inset: Corresponding UV–Vis DRS Spectrum

form elemental distribution and high crystallinity, suggests that the Nb_2O_5_72h sample has matured into a structurally robust and compositionally homogeneous material (Taher et al., 2021b). These features are expected to contribute positively to its performance in photocatalytic or adsorption-based environmental applications

The specific surface area and porosity characteristics of the Nb_2O_5_72h sample were investigated using nitrogen adsorpti on-desorption isotherms, as shown in Figure 3. The isotherm profile exhibits a typical type IV curve with a hysteresis loop in the relative pressure range of 0.4 – 0.9, indicative of mesoporous structures (Kouznetsova et al., 2019). The Brunauer-Emmet-Telle (BET) analysis reveals a high surface area of 242.43 m^2/g, which is significantly larger than those of conventional Nb_2O_5 materials reported in the literature ((Athar et al., 2012; Huang et al., 2016). The Barett-Joyner-Halenda (BJH) pore size distribution (inset) shows a predominant mesopores range centered around 10 – 15 nm, which is favorable for molecular diffusion and enhanced photocatalytic activity.

The optical properties of Nb_2O_5_72h sample were further examined by UV-Vis diffuse reflectance spectroscopy (DRS), and the band gap energy (Eg) was estimated using the Tauc plot method. (Figure 4b). The absorption edge appears near 380 nm, and the extrapolation of the linear region of the (F(R)hv) 0.5 plot yield an optical band gap of 3.28 eV. This value is consistent with that orthorhombic Nb2O5 and confirms its intrinsic semiconducting nature (Taher et al., 2021b). Although the band gap lies within the UV range, the high surface area and mesoporosity may synergistically enhance light absorption, charge carrier separation, and surface reactions kinetics.

Table 1. Comparison of Adsorption Capacities of Various Materials Reported in Literature for Tetracycline (TC) Removal

Materials	Adsorption capacity (mg/g)	References
N-doped TiO_2	27.82	(Zou et al., 2018)
MIL-125(Ti)	41.4	(Dai et al., 2025)
TP207	5.039	(Gong et al., 2022)
Orthorhombic Nb_2O_5	32.3	This work

3.2 Adsorption and Photocatalytic Activity

Figure 4a illustrates the effectiveness of *ortho*-Nb_2O_5 in removing tetracycline (TC) under both dark conditions (adsorption) and ultraviolet (UV) irradiation (photocatalysis). The results indicate that ortho-Nb2O5 exhibits significant adsorption properties and notable photocatalytic activity. This performance surpasses several previously reported multifunctional materials that exhibit both adsorption and photocatalytic activity. A comparison of adsorption capacities from related studies is summarized in Table 1, highlighting the competitive efficiency of the synthesized *ortho*-Nb_2O_5 in removing tetracycline from aqueous environments. Based on the obtained kinetic modeling (Figures 4b-d), it followed the pseudo-second-order model (Rianjanu et al., 2024b). This suggests that the adsorption process was chemically controlled through surface interactions rather than simply physical sorption. After reaching the equilibrium

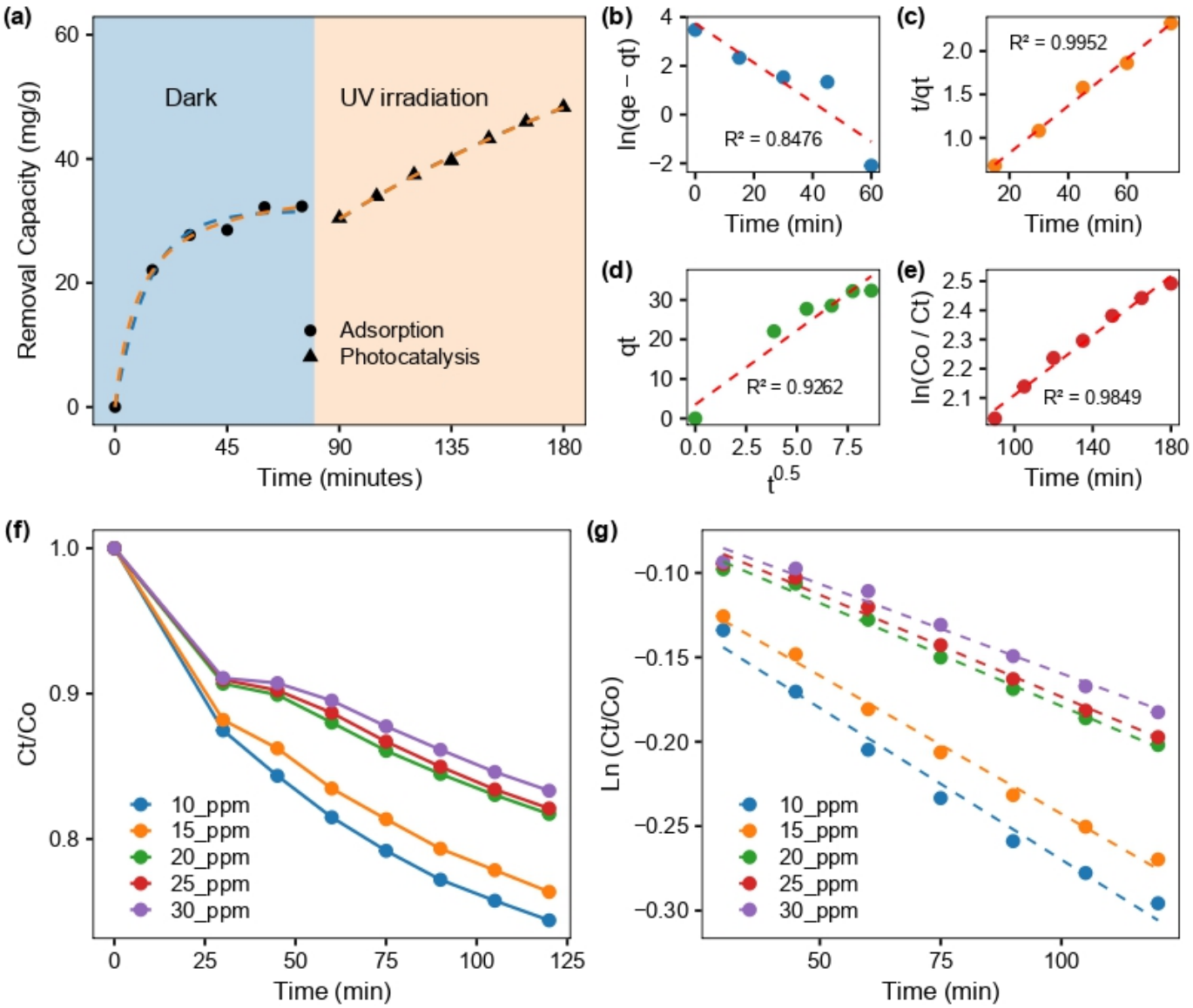

Figure 4. Adsorption and Photocatalytic Degradation of Tetracycline Using Nb_2O_5. (A) Effect of Contact Time Under Dark (Adsorption) and UV Irradiation (Photocatalysis). (B) Pseudo-First Order (PFO) Kinetic Model for Adsorption. (C) Pseudo-Second Order (PSO) Kinetic Model for Adsorption. (D) Langmuir-Hinshelwood Kinetic Model for Photocatalytic Degradation

removal capacity under dark conditions (75 min), additional removal capacity was achieved when the reactor was irradiated with UV light, reaching 48 mg/g within 180 minutes. Pseudo-first-order kinetics modeling was applied to the obtained data, indicating a good fit (Figure 4e).

The further photocatalytic degradation of TC over *ortho*-Nb_2O_5 was investigated at various initial concentrations (10, 15, 20, and 25 mg/L) to assess the impact of pollutant loading on degradation efficiency. As shown in Figure 4f, the photocatalytic degradation efficiency decreases as TC concentration increases. This trend can be attributed to the greater availability of active sites and lower molecular competition at reduced TC concentrations, which facilitates more effective interactions between the pollutant and the catalyst surface (Taher et al., 2021b).

Upon UV light irradiation, the *ortho*-Nb_2O_5 photocatalyst is activated by absorbing photons with energy equal to or greater than its band gap (~3.28 eV), leading to the excitation of electrons (e^-) from the valence band to the conduction band and the simultaneous formation of holes (h^+) in the valence

band. These charge carriers subsequently participate in redox reactions where the photogenerated holes can directly oxidize tetracycline molecules or react with surface-adsorbed water to generate highly reactive hydroxyl radicals (•OH). Meanwhile, the excited electrons reduce dissolved oxygen molecules to form Superoxide radicals ($•O_2^-$). Both •OH and $•O_2^-$ are key reactive oxidative species (ROS) that contribute to the degradation of TC into less harmful intermediates or complete mineralization products. This proposed mechanism is consistent with previous findings on Nb_2O_5-based photocatalysts (Rianjanu et al., 2024a).

4. CONCLUSIONS

This study demonstrates the potential of hydrothermally synthesized *ortho*-Nb_2O_5 as a bifunctional material for tetracycline removal through adsorption and photocatalysis. The optimized *ortho*-Nb_2O_5 exhibited a high surface area, mesoporosity, and a suitable band gap (3.28 eV), enabling efficient UV-driven photocatalysis. Adsorption studies followed pseudo-second-order kinetics, suggesting chemisorption, while photocatalytic degradation was well-fitted to a pseudo-first-order model. The material's dual functionality makes it a promising candidate for sustainable wastewater treatment applications.

5. ACKNOWLEDGMENT

The author would like to express sincere gratitude to Institut Teknologi Sumatera for providing financial support for this research through the GBU 45 Research Grant, under contract number 631g/IT9.2.1/PT.01.03/2023. This support has been instrumental in the successful completion of this study.

REFERENCES

Ahmad, I., A. Al-Qattan, M. Z. Iqbal, A. Anas, M. A. Khasawneh, A. J. Obaidullah, A. Mahal, M. Duan, W. Al Zoubi, Y. Y. Ghadi, N. Al-Zaqri, and C. Xia (2024). A Systematic Review on Nb_2O_5-Based Photocatalysts: Crystallography, Synthetic Methods, Design Strategies, and Photocatalytic Mechanisms. *Advances in Colloid and Interface Science*, **324**; 103093

Almansour, A., N. J. Ahmed, and M. Yousfan (2021). A Retrospective Surveillance of Antibiotic Use in the Intensive Care Unit in a University Hospital in North Cyprus. *Latin American Journal of Pharmacy*, **40**(2); 274–278

Antos, J., M. Piosik, D. Ginter-Kramarczyk, J. Zembrzuska, and I. Kruszelnicka (2024). Tetracyclines Contamination in European Aquatic Environments: A Comprehensive Review of Occurrence, Fate, and Removal Techniques. *Chemosphere*, **353**; 141519

Asif, M., M. Latif, J. Yang, R. Wahab, B. Rasool, and M. H. Aziz (2024). Visible Light Driven Photocatalyst $NiFe_2O_4/Ag_2WO_4$ Nanocomposite for the Degradation of Tetracycline (TC-HCl) Antibiotics. *Materials Letters*, **377**; 137391

Athar, T., A. Hashmi, A. Al-Hajry, Z. A. Ansari, and S. G. Ansari (2012). One-Pot Synthesis and Characterization of Nb_2O_5 Nanopowder. *Journal of Nanoscience and Nanotechnology*, **12**(10); 7922–7926

Daghrir, R. and P. Drogui (2013). Tetracycline Antibiotics in the Environment: A Review. *Environmental Chemistry Letters*, **11**(3); 209–227

Dai, Q., G. Gao, J. Tang, R. Jiang, S. Sun, Y. Ye, S. Li, R. Xie, and J. Zhang (2025). The MIL-125(Ti)/Co_3O_4 Towards Efficiently Removing Tetracycline by Synergistic Adsorption-Photocatalysis Roles. *Materials & Design*, **250**; 113608

Filliping, L., Z. Yi, and H. Yingping (2008). Determination of Tetracycline Antibiotics in the Environmental Samples. *Progress in Chemistry*, **20**(12); 2075–2082

Gong, Y., Y. Wang, M. Tang, H. Zhang, P. Wu, C. Liu, J. He, and W. Jiang (2022). A Two-Step Process Coupling Photocatalysis With Adsorption to Treat Tetracycline–Copper(II) Hybrid Wastewaters. *Journal of Water Process Engineering*, **47**; 102710

Hamdan, A., M. N. AbuHaweeleh, L. Al-Qassem, A. Kashkoul, I. Alremawi, U. Hussain, S. Khan, M. M. S. ElBadway, T. Chivese, H. H. Farooqui, and S. M. Zughaier (2024). Prevalence of Antimicrobial Resistance Among the WHO's AWaRe Classified Antibiotics Used to Treat Urinary Tract Infections in Diabetic Women. *Antibiotics*, **13**(12); 1218

Haseeb, A., S. S. A. Abuhussain, S. Alghamdi, S. M. Bahshwan, A. J. Mahrous, Y. A. Alzahrani, A. F. Alzahrani, A. AlQarni, M. AlGethamy, A. S. Naji, A. A. O. Khogeer, M. S. Iqbal, B. Godman, and Z. Saleem (2023). Point Prevalence Survey of Antimicrobial Use and Resistance During the COVID-19 Era Among Hospitals in Saudi Arabia and the Implications. *Antibiotics*, **12**(11); 1609

Huang, C., J. Fu, H. Song, X. Li, X. Peng, B. Gao, X. Zhang, and P. K. Chu (2016). General Fabrication of Mesoporous Nb_2O_5 Nanobelts for Lithium Ion Battery Anodes. *RSC Advances*, **6**(93); 90489–90493

Koundle, P., N. Nirmalkar, M. Momotko, S. Makowiec, and G. Boczkaj (2024). Tetracycline Degradation for Wastewater Treatment Based on Ozone Nanobubbles Advanced Oxidation Processes (AOPs) – Focus on Nanobubbles Formation, Degradation Kinetics, Mechanism and Effects of Water Composition. *Chemical Engineering Journal*, **501**; 156236

Kouznetsova, T. F., A. I. Ivanets, and V. S. Komarov (2019). Low-Temperature Synthesis of Mesoporous M41S Metal-Silicates and Their Adsorption and Capillary-Condensation Properties. *Proceedings of the National Academy of Sciences of Belarus, Chemical Series*, **55**(3); 338–344

Leong, C. Y., H. L. Teh, M. C. Chen, and S. L. Lee (2022). Effect of Synthesis Methods on Properties of Copper Oxide Doped Titanium Dioxide Photocatalyst in Dye Photodegradation of Rhodamine B. *Science and Technology Indonesia*, **7**(1); 91–97

Mishra, P., G. Tripathi, V. Mishra, T. Ilyas, S. Firdaus, S. Ahmad, A. Farooqui, N. Yadav, S. Rustagi, S. Shreaz, R. Negi, and A. N. Yadav (2025). Antibiotic Contamination in

Wastewater Treatment Plant Effluents: Current Research and Future Perspectives. *Environmental Nanotechnology, Monitoring and Management*, **23**; 101047

Nakajima, K., J. Hirata, M. Kim, N. K. Gupta, T. Murayama, A. Yoshida, N. Hiyoshi, A. Fukuoka, and W. Ueda (2017). Facile Formation of Lactic Acid from a Triose Sugar in Water over Niobium Oxide with a Deformed Orthorhombic Phase. *ACS Catalysis*, **8**(1); 283–290

Ni, Q., X. Ke, W. Qian, Z. Yan, J. Luan, and W. Liu (2024). Insight into Tetracycline Photocatalytic Degradation Mechanism in a Wide pH Range on BiOI/BiOBr: Coupling DFT/QSAR Simulations With Experiments. *Applied Catalysis B: Environmental*, **340**; 123226

Nie, Y., T. Zhang, Y. Xu, Y. Du, J. Ai, and N. Xue (2024). Study on Mechanism of Removal of Sudden Tetracycline by Compound Modified Biological Sand Filtration Process. *Journal of Environmental Management*, **356**; 120709

Rianjanu, A., K. D. P. Marpaung, E. K. A. Melati, R. Aflaha, Y. G. Wibowo, I. P. Mahendra, N. Yulianto, J. Widakdo, K. Triyana, H. S. Wasisto, and T. Taher (2024a). Integrated Adsorption and Photocatalytic Removal of Methylene Blue Dye From Aqueous Solution by Hierarchical Nb_2O_5@PAN/PVDF/ANO Composite Nanofibers. *Nano Materials Science*, **6**(1); 96–105

Rianjanu, A., K. D. P. Marpaung, C. Siburian, S. A. Muhtar, N. I. Khamidy, J. Widakdo, N. Yulianto, R. Aflaha, K. Triyana, and T. Taher (2024b). Enhancement of Photocatalytic Activity of CeO_2 Nanorods Through Lanthanum Doping (La–CeO_2) for the Degradation of Congo Red Dyes. *Results in Engineering*, **23**; 102748

Rivera-Utrilla, J., R. Ocampo-Pérez, M. Sánchez-Polo, J. J. López-Peñalver, and C. V. Gómez-Pacheco (2018). Removal of Tetracyclines From Water by Adsorption/Bioadsorption and Advanced Oxidation Processes: A Short Review. *Current Organic Chemistry*, **22**(10); 1005–1021

Saadati, F., N. Keramati, and M. M. Ghazi (2016). Influence of Parameters on the Photocatalytic Degradation of Tetracycline in Wastewater: A Review. *Critical Reviews in Environmental Science and Technology*, **46**(8); 757–782

Santos, K. M. A., E. M. Albuquerque, T. L. Coelho, and M. A. Fraga (2021). Continuous Aqueous-Phase Cascade Conversion of Trioses to Lactic Acid over Nb_2O_5 Catalysts. *Biomass Conversion and Biorefinery*, **13**(13); 11865–11878

Serwecińska, L. (2020). Antimicrobials and Antibiotic-Resistant Bacteria: A Risk to the Environment and to Public Health. *Water (Switzerland)*, **12**(12); 3313

Taher, T., R. Putra, N. Rahayu Palapa, and A. Lesbani (2021a). Preparation of Magnetite-Nanoparticle-Decorated NiFe Layered Double Hydroxide and Its Adsorption Performance for Congo Red Dye Removal. *Chemical Physics Letters*, **777**; 138712

Taher, T., A. Yoshida, A. Lesbani, I. Kurnia, G. Guan, A. Abudula, and W. Ueda (2021b). Adsorptive Removal and Photocatalytic Decomposition of Cationic Dyes on Niobium Oxide With Deformed Orthorhombic Structure. *Journal of Hazardous Materials*, **415**; 125635

Thakur, R., A. Singh, R. Dhanwar, S. Kadam, U. Waghmare, T. Lodha, B. S. Lopes, and O. Prakash (2025). Global Perspectives on Residual Antibiotics: Environmental Challenges and Trends. *Discover Sustainability*, **6**(1); 232

Wang, X., W. Li, R. Harrington, F. Liu, J. B. Parise, X. Feng, and D. L. Sparks (2013). Effect of Ferrihydrite Crystallite Size on Phosphate Adsorption Reactivity. *Environmental Science & Technology*, **47**(18); 10322–10331

Yao, J., X. Tong, S. Lu, Y. Meng, and G. Li (2024). Photocatalytic Degradation of Tetracycline Over Bimetallic Layered Double Hydroxides–MXenes Heterostructures Under Visible Light. *Materials Letters*, **375**; 137242

Zou, Y., X. Hu, H. Cao, and Y. Ruan (2018). Adsorption Performance of N-Doped TiO_2 Nanomaterials for Tetracycline Hydrochloride Wastewater. *Lizi Jiaohuan Yu Xifu / Ion Exchange and Adsorption*, **34**(1); 63–73

